Nafion®/polystyrene-b-poly(ethylene-ran-butylene)-b-polystyrene composite membranes with electric field-aligned domains for improved direct methanol fuel cell performance

X. Wei, M.Z. Yates*

Department of Chemical Engineering, University of Rochester, Rochester, NY 14627, United States

ABSTRACT

Composite membranes were fabricated consisting of aligned domains of Nafion® 1100 surrounded by a supporting matrix of polystyrene-b-poly(ethylene-ran-butylene)-b-polystyrene (SEBS). The structure of the composite was controlled via the application of an electric field during solvent casting. Nafion® domains were aligned across the membrane thickness to provide paths for proton conduction. The surrounding SEBS domain limits methanol permeability. Compared to randomly structured Nafion®/SEBS composites, the membranes with field-aligned domains display significantly enhanced performance in direct methanol fuel cells (DMFCs). The membranes with field-aligned domains display DMFC performance better than commercial Nafion® 117 membranes under high methanol fuel concentration.

© 2009 Elsevier B.V. All rights reserved.

1. Introduction

Methanol is attractive as a high energy density liquid fuel that can be used directly in fuel cells without reforming [1,2]. One of the main challenges currently limiting performance of direct methanol fuel cells (DMFCs) is the high permeability of most common polymeric fuel cell membranes to methanol. Perfluorinated sulfonated polymers such as Nafion® are commonly used as fuel cell membrane materials because they have high proton conductivity, mechanical strength, and chemical stability under typical fuel cell operating conditions. Protons are transported through sulfonated polymer membranes such as Nafion® primarily in the form of H_3O^+ ions [3]. As a result, the membranes must be swollen with water in order to function effectively in fuel cells. While water sorption enhances proton conductivity in sulfonated polymers, it also increases methanol fuel crossover since water and methanol are transported through the membranes together [4,5]. When methanol passes through the membrane from the anode to the cathode, the loss of fuel lowers fuel cell voltage and efficiency. Studies of DMFCs operating with Nafion® 117 membranes reported that more than 35% of the methanol was lost by crossover through the membrane [6–8].

Several different approaches have been taken to improve DMFC membrane performance, including the development of new poly-

mers, chemical modification of conventional polymers, and the preparation of composite membranes [4,9–11]. In composite DMFC membranes, functional particles can be added to a polymer to improve fuel cell performance. For example, particles that act as methanol barriers can lower methanol permeability and limit swelling of proton conducting polymers [12,13]. Alternatively, proton conducting particles can be added to a polymer having good methanol barrier properties in order to enhance conductivity [10,14,15]. The transport properties of composite membranes are highly dependent on the spatial arrangement of the functional particles, including particle volume fraction, size, shape, orientation, and connectivity between particles.

In the present study, we investigate the DMFC performance of composite membranes in which composite structure is controlled through the application of an electric field during membrane formation. Under appropriate conditions, an electric field applied to a suspension of particles in a liquid will induce particles to align into connected chains in the direction of the field lines [16–19]. The particle chaining phenomenon occurs when the particles have a higher dielectric constant than the surrounding liquid, i.e. positive dielectrophoresis is required [18,19]. Particle chaining can be exploited to create polymer/particle composites with anisotropic properties by chaining particles suspended in a liquid and solidifying the composite to fix the field-induced structure through chemical reaction or a change in temperature [20–25]. We recently demonstrated the creation of proton conducting membranes with enhanced transport properties by electric field induced chaining of sulfonated poly(ether ether ketone) particles in a thermally curable silicone

---

* Corresponding author. Tel.: +1 585 273 2335; fax: +1 585 273 1348.
E-mail address: myates@che.rochester.edu (M.Z. Yates).

resin [24]. We also recently demonstrated the enhancement of proton conductivity in Nafion®/poly(vinylidene fluoride) composites through applying an electric field during a novel polymer melt process [25]. Neither of these proton conducting membranes were directly usable in fuel cells, however. The silicone-based membranes have high oxygen permeability and the poly(vinylidene fluoride)-based membranes are too thick, increasing resistance to proton transport.

In order to make thin composite membranes suitable for DMFC application, the goal of the present study is to control composite structure through the application of electric fields during solvent casting. The solvent casting process involves evaporating solvent from a polymer solution and is commonly employed to create thin polymeric and polymer composite fuel cell membranes [9,13]. To date, there has been no report of using electric fields to control the structure of composite membranes made by solvent casting. Convective currents and film thinning from solvent evaporation can potentially disrupt the electric field induced structure. In addition, solvent evaporation requires processing conditions with an open air gap between one of the electrodes and the particle suspension to allow solvent vapor to escape. Since proton conducting polymers are typically only soluble in high dielectric constant solvents, the majority of the electric field potential will be lost across the air gap and particles will not respond to the applied field.

In the present study we chose polystyrene-b-poly(ethylene-ran-butylene)-b-polystyrene (SEBS) as the membrane forming polymer. SEBS is an inexpensive thermoplastic elastomer with excellent mechanical flexibility and chemical stability. There are several literature reports demonstrating the application of sulfonated SEBS in fuel cells [26–28]. SEBS was chosen because it is soluble in low dielectric constant solvents such as toluene and xylene. Here we show that proton conducting particles suspended in SEBS/p-xylene solutions easily form chains under an applied field even when an air gap is between one of the electrodes and the particle suspension. By solvent casting under an applied electric field, the structure of the composite membranes can be altered by particle chaining and membrane thickness can easily be adjusted. The field-induced structure results in Nafion®/SEBS composites with significantly enhanced transport properties and improved DMFC performance.

2. Experimental

2.1. Materials

SEBS powder ($M_w \sim 118,000 \, \mathrm{g \, mol^{-1}}$) and p-xylene (99%, ReagentPlus) were purchased from Sigma–Aldrich. Nafion® 117 membranes and Nafion® 1100 dispersions (15 wt.% and 20 wt.% in an isopropanol/water mixture) were purchased from Ion Power. Nafion® particles were obtained by drying a 15 wt.% Nafion® dispersion in a vacuum oven at 80 °C for 1 day, then grinding into a fine powder with a mortar and pestle. The powder was sieved to obtain particles less than 45 μm in size. The morphology of the particles was observed by scanning electron microscopy (SEM), as shown in Fig. 1.

2.2. Observation of particle response to the applied electric field

Two custom cells were designed to observe the Nafion® particle response to the applied electric fields using optical microscopy. The first cell consists of two parallel aluminum electrodes attached to a glass microscopy slide, as shown in Fig. 2. The particle suspension was transferred via pipette to the surface of the non-ground electrode leaving a space between the suspension and the ground electrode. An air gap of ~4–5 mm separated the ground electrode from the edge of the liquid suspension. This cell allowed side-view
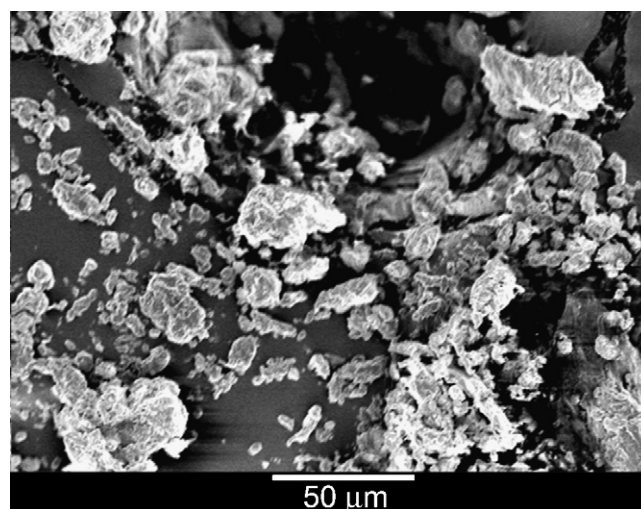

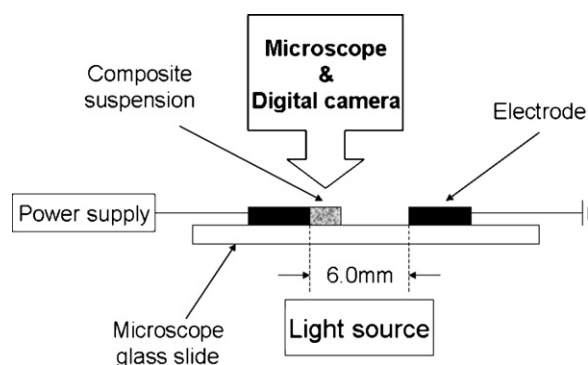**Fig. 1.** SEM image of Nafion® particles.

Fig. 2. Experimental setup for side-view observation of particle response to an applied electric field.

imaging of particle chaining induced by the electric field. A second cell was constructed for top-view imaging of chaining. Fig. 3 shows the cell, consisting of two parallel transparent indium-tin-oxide (ITO) coated electrodes held 6 mm apart using Teflon spacers. The particle suspension ~1 mm thick was held in a Teflon frame, leaving ~5 mm air gap between the upper (ground) electrode and the surface of the liquid film.
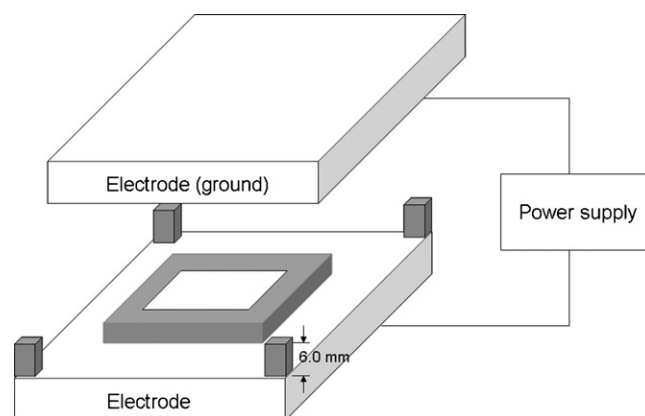

Fig. 3. Experimental setup for top-view observation of particle response to an applied electric field.

2.3. Membrane preparation

Composite membranes were formed from dispersions of Nafion® particles in 15 wt.% SEBS solution in *p*-xylene. Ultrasonic energy (VWR Aquasonic Cleaner 75T) and mechanical stirring were applied for 2 h to disperse Nafion® particles as a homogeneous suspension in SEBS solution. The amount of Nafion® suspended in the SEBS solution was varied from 10 wt.% to 70 wt.%. Solvent casting of membranes from the suspension under applied electric field was carried out in the custom cell shown in Fig. 3. The Teflon frame was filled with the Nafion®/SEBS suspension and left in a fume hood at room temperature for 3 h to remove the solvent with or without an applied alternating current electric field of 6 kV at 1 kHz. The membranes were dried in a vacuum oven overnight at 80 °C to remove any residual solvent. The membranes were treated at 80 °C with 3 wt.% H_2O_2, deionized water, 5 wt.% H_2SO_4, and then deionized water again successively for 1 h each. For comparison, Nafion® 117 membranes were pre-treated using the same method. All membranes were kept in deionized water before other testing.

2.4. Membrane characterization

Membranes were dried at 80 °C under vacuum and water uptake was measured from the percentage increase in weight after soaking in deionized water to the fully hydrated state at room temperature. Dimensional change was measured using a micrometer from the percentage increase in the through-plane and in-plane directions of the membrane after soaking it in 2 M and 8 M CH_3OH for 3 days. Methanol permeability of water-saturated membranes was measured by gas chromatography (Hewlett Packard model 5890A). The membrane was clamped between two 30 ml reservoirs using a custom made glass permeability cell. One reservoir was filled with 2 M methanol and the other with deionized water. The permeability was determined from measured methanol concentration versus time at room temperature from samples taken from the reservoir initially filled with deionized water. An approximate solution of the continuity equation for diffusion in plane sheet geometry at early times was used to estimate permeability [7,8,10]. Through-plane proton conductivity of water-saturated membranes was measured at room temperature by the two-point probe method using a Gamry PCI4/750 potentiostat over the frequency region from 1 Hz to 300 kHz. The conductivity was calculated from the bulk resistance of the membrane, which was determined from real values in Nyquist plot by extrapolating of impedance arcs [29,30].

2.5. Fuel cell performance test

Catalyst inks were prepared by mixing 60% Pt/C (E-Tek, for cathode) or 60% PtRu/C (E-Tek, developmental catalyst, atomic ratio 1:1, for anode) with Nafion® dispersion. For both anode and cathode, the weight ratio of catalyst to Nafion® was 3:1. To fabricate the membrane electrode assembly (MEA), the catalyst inks were brushed onto a carbon cloth (E-Tek) as the electrode substrate. Numerous thin layers of the catalyst ink were successively applied onto the substrate at 60 °C and each layer was dried for 3 min before another one was brushed on [31]. The catalyst loading was 2 mg cm^{-2} and 3 mg cm^{-2} for the cathode and anode, respectively. To improve catalyst utilization, a thin layer of Nafion® (∼10 μm) was applied to the surface to the composite membranes by dip coating in a 1 wt.% Nafion® dispersion [15,32]. The MEAs were fabricated by hot pressing at 130 °C and ∼900 psig. Polarization curves were collected using a single-cell test station (Scribner Series 850C) with a working area of 5 cm^2. Aqueous methanol solution at the anode was supplied by a peristaltic pump (Gilson Minipulse 3) at a flow rate of 1 ml min^{-1} while the cathode was fed with humidified air at 500 ml min^{-1}. Prior to performance testing, the cell was con-ditioned at constant current density operation (20–80 mA cm^{-2}) until polarization curves collected at time intervals of 1 h showed no change.

3. Results and discussion

The desired electric field induced chaining of Nafion® particles requires that the particles be suspended in a liquid medium of lower polarizability than the particles [18,19]. The dielectric constant of dry Nafion® is approximately 4 [33]. We chose SEBS as the membrane forming polymer because it can be solvent cast from solutions of low dielectric constant. Solutions of SEBS dissolved in xylene have a dielectric constant between 2 and 3 [34,35]. To confirm particle chaining, Nafion® particles were dispersed in a SEBS/*p*-xylene solution, and observations were made through optical microscopy on particle suspensions as electric fields were applied. Two different electrode arrangements were used, as shown in Figs. 2 and 3. For both types of electrode arrangements, there is an air gap of 4–5 mm between the ground electrode and the liquid surface of the particle suspension to allow solvent vapor to escape. Since Nafion® particles have a net electrostatic charge, they will migrate by electrophoresis if a direct current field is applied. To avoid electrophoresis, alternating current fields were applied with a fixed frequency of 1 kHz. This frequency was found to be effective in a similar prior study [24]. Particle alignment was observed as the field strength was varied. It was found that as the field strength was increased, an increasing fraction of the particles was aligned into chains. The time required to form chains was reduced as field strength is increased, consistent with our previous study [24]. When the field was below 100 V mm^{-1}, there was no obvious change after applying the field for 1 min. As field strength was increased above 500 V mm^{-1}, particles were observed to rapidly migrate into chains within a few seconds. Fig. 4 shows the particles before and after applying an electric field of 1 kV mm^{-1} for 10 s. For the electrode geometry in Fig. 2, the particle chains form perpendicular to the direction of observation. The chains form parallel to the direction of observation for the electrode geometry in Fig. 3. Fig. 4 confirms that the Nafion® particle chains are aligned in the direction of the applied electric field lines.

Membrane formation was investigated by solvent casting dispersions of Nafion® particles in SEBS solutions in *p*-xylene. For membrane formation, the electrode cell shown in Fig. 3 was used to align Nafion® particles in chains aligned through the membrane thickness direction for optimizing proton transport. Membranes were formed by solvent evaporation at room temperature for 3 h while maintaining an applied field of 1 kV mm^{-1} at 1 kHz. For comparison, parallel experiments were carried out without the applied field. In order to reduce particle sedimentation while still allowing the particles to move in response to the applied field, viscous 15 wt.% SEBS solutions were chosen to prepare composite membranes when the Nafion® concentration was varied from 0 wt.% to 50 wt.%. As Nafion® content was increased to 70 wt.%, less viscous 10 wt.% SEBS solution was used to allow Nafion® particles to move in response to the applied field. The amount used for solvent casting was adjusted by trial and error to give a membrane thickness of ∼140 μm as measured by digital micrometer. There was no significant difference in thickness between the field-aligned and non-aligned membranes. All composite membranes showed excellent mechanical flexibility and appeared to have particles uniformly distributed over the membrane area.

The chemical stability of the membranes was investigated using Fenton's reagent test, a standard method for predicting chemical stability in an operating fuel cell [36]. Since the stability of Nafion® in Fenton's reagent is well investigated, we only tested the pure SEBS membrane. A pure SEBS membrane ∼140 μm thick-
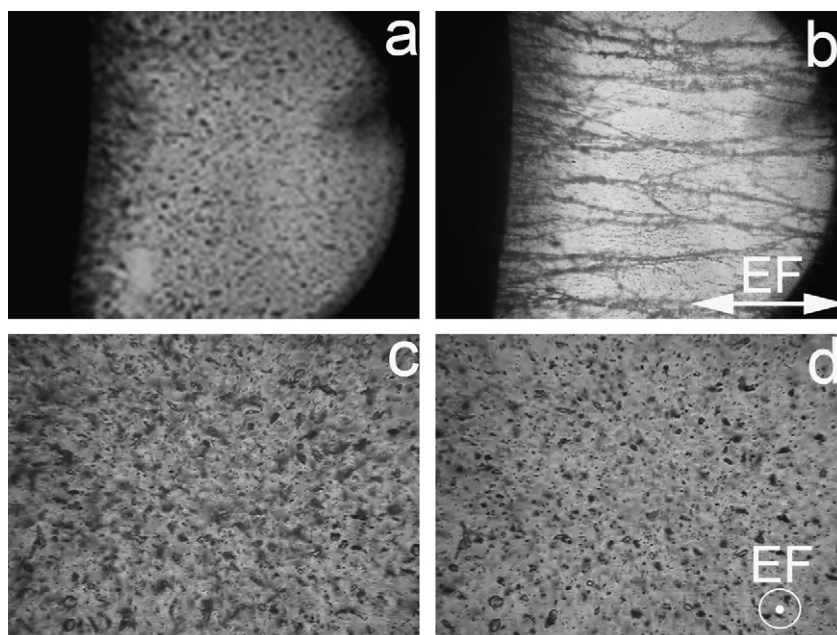
Fig. 4. Optical microscopy images of composite Nafion®/SEBS/p-xylene suspensions: (a) side-view before applying field; (b) side-view after applying field; (c) top-view before applying field; (d) top-view after applying an electric field.

ness formed by solvent casting at room temperature from a 15 wt.% solution in p-xylene was suspended in Fenton's reagent at 68 °C. The membrane had no measurable loss in weight after 2 days of continuous testing, indicating that SEBS is chemically stable against oxidation by Fenton's reagent. In addition, the SEBS membrane had no noticeable change in appearance, mechanical strength, or flexibility after the Fenton's test, based on visual observation while manually bending the membrane. The Fenton's test suggests that SEBS membranes will show good chemical stability in operating fuel cells.

The thermal stability of the Nafion®/SEBS composite membranes was investigated by thermogravimetric analysis (TGA). Fig. 5 shows the TGA curves for the Nafion® particles, SEBS and 50/50 Nafion®/SEBS composite membranes formed with or without the applied field (Nafion®/SEBS-EF and Nafion®/SEBS-No EF, respectively). The TGA curves were obtained by heating in nitrogen from room temperature at a rate of 10 °C min^{-1} using TA instruments DSC/TGA model Q600. The results show that SEBS has an approximate degradation temperature of 430 °C. The Nafion® particles show a gradual weight loss about 6.3% from room temperature to 290 °C, which is attributed to dehydration. Between 290 °C and 560 °C, Nafion® has a three-stage degradation pattern: desulfonation (290–400 °C), side-chain decomposition (400–470 °C) and

PTFE backbone decomposition (470–560 °C) [37]. For the composite membranes, the degradation process starts from 290 °C similar to that of Nafion®. The field applied membrane shows early dehydration with the weight loss of water of 2.7% compared to 2.4% for non-aligned membrane. The TGA curves for the 50/50 composite membranes lie between the two pure components, but close to that of SEBS. It is possible that SEBS acts as a barrier to retard the dehydration of Nafion® particles, especially when the particles are randomly dispersed into the SEBS matrix.

The proton conductivity and methanol permeability of fuel cell membranes are closely related to water uptake capacity. Swelling of the membranes with water is a requirement for proton conductivity, but also enhances methanol permeability. Swelling can also impart mechanical stress on the membranes that can lead to fuel cell device failure [38]. Membrane swelling was determined by measuring the increase in weight of dry membranes after submersion in deionized water until reaching constant weight. Pure Nafion® 117 membranes were measured to take up 26.4 wt.% water at room temperature, which is in agreement with literature report [39]. Pure SEBS has no water uptake. Fig. 6 shows the swelling behavior of a series of composite SEBS membranes of varying Nafion® content. As Nafion® is added to the SEBS, the water uptake
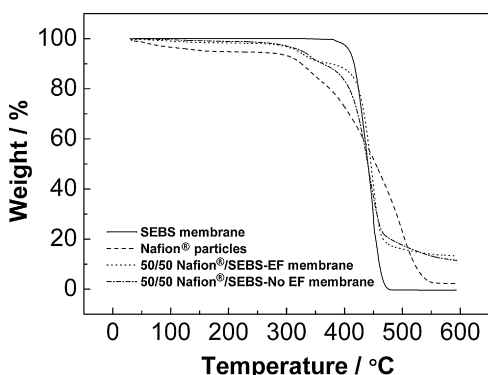

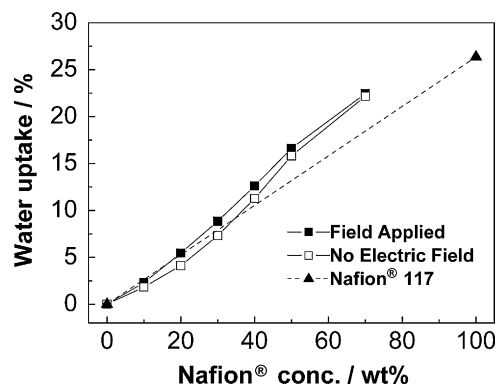**Fig. 5.** TGA curves of Nafion®, SEBS and 50/50 composite membranes.

Fig. 6. Water uptake plots for membranes with and without the applied electric field.
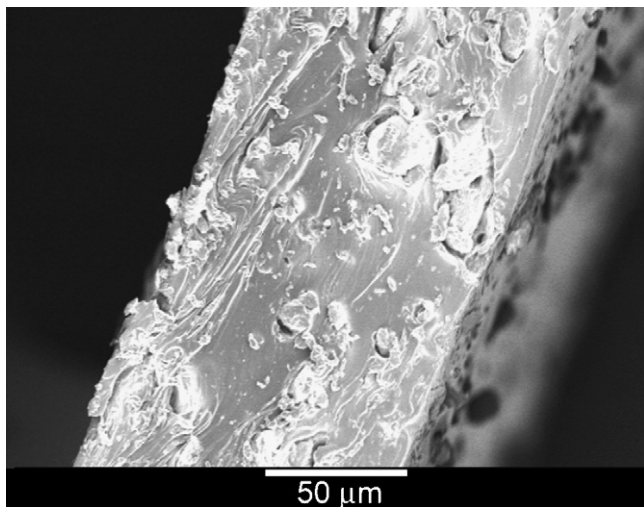
Fig. 7. Cross-sectional morphology of 40 wt.% Nafion®/SEBS membrane formed without the applied field.

Fig. 8. Dimensional change of Nafion®/SEBS due to swelling by 2 M and 8 M methanol at room temperature as function of Nafion® content.

increases as expected. All membranes with electric field-aligned Nafion® particles displayed higher water uptake than the randomly structured membranes having the same Nafion® content. By aligning Nafion® particles into chains, more of the Nafion® is accessible to water. The randomly structured composites likely have some fraction of the Nafion® particles completely surrounded by SEBS, blocking access to water. If all Nafion® particles were accessible to water, it is expected that the water swelling as a function of Nafion® content would be linear. However, Fig. 6 shows water swelling as a function of Nafion® content appears sigmoidal. At low Nafion® loading, the SEBS can block access of some particles to water and potentially constrain swelling. As a result, the swelling is lower than it would be if all Nafion® particles were accessible to water and swell the same as bulk Nafion®. At higher Nafion® content, the composite membranes uptake more water than is expected based on the Nafion® loading. The excess water uptake measured at higher Nafion® loading is likely due to capillary filling of void spaces at the Nafion®/SEBS interface. A cross-sectional side-view image of a membrane is shown in Fig. 7. There appears to be some void spaces between the Nafion® and SEBS phases that could account for the excess swelling measured in Fig. 6. Composites made from immiscible materials often have such voids at the interfaces between the two domains. However, this discrete interface maybe leads to poor mechanical properties in comparison with the two dense components. Our future studies are focused on the composite systems that have miscible materials.

The dimensional changes of membranes due to swelling leads to mechanical stress that can cause interfacial delamination of the electrodes from the membrane surface in an operating fuel cell, resulting in dramatic degradation of the cell performance [40]. Fig. 8 shows the dimensional change of the composite membranes and Nafion® 117 after swelling in 2 M and 8 M methanol solutions at room temperature. The expansion of the composite membranes increases with increasing Nafion® content and methanol concentration for both aligned and non-aligned membranes. The swelling of pure Nafion® results in about 17% and 23% increases in length of a Nafion® 117 membranes using 2 M and 8 M methanol solutions respectively. The composite membranes display significantly smaller dimensional changes than pure Nafion®. When Nafion® content is 50 wt.%, the change in length due to swelling is less than half of that of pure Nafion® for the membrane formed under the applied electric field. Moreover, the membranes formed under the applied electric field have smaller changes in length compared to membranes with the same Nafion® content formed without
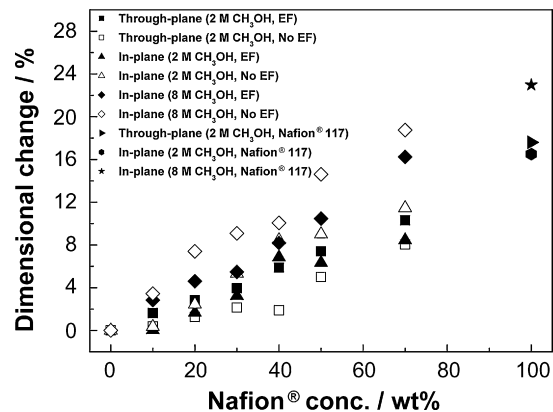
the applied field, particularly at high methanol concentration. The 50/50 aligned membrane shows only around 10% increase in length compared to 15% for the non-aligned membrane when soaking in 8 M methanol solutions. The swelling results show that the electric field-induced structure results in anisotropic swelling behavior, with the electric field processed membranes having enhanced thickness expansion and reduced area expansion. Minimizing the membrane area expansion is critical to reducing the forces that lead to electrode delamination in fuel cells undergoing cycling in relative humidity.

The proton conductivity of a series of membranes made with varying Nafion® content is shown in Fig. 9. The two-point probe method was used to measure through plane conductivity of fully water-saturated membranes. The results show that proton conductivity increases with increasing Nafion® content in the composites. The electric field-aligned membranes display higher conductivity than membranes with randomly dispersed particles at the same Nafion® content. The proton conductivity results are consistent with the measured higher water uptake for the electric field-aligned membranes compared to randomly structured membranes at the same Nafion® content. The electric field induced chaining creates paths for proton transport through the membrane. Isolated Nafion® domains that are completely surrounded by SEBS cannot effectively participate in proton conduction. Therefore, proton conductivity is much lower for randomly dispersed Nafion® particles, particularly at low particle concentration. As Nafion® content is increased even the randomly dispersed particles begin to form a connected network to provide proton transport paths through the membrane. When the Nafion® content is 70 wt.%, membranes formed with and without the applied field show similar conductiv-
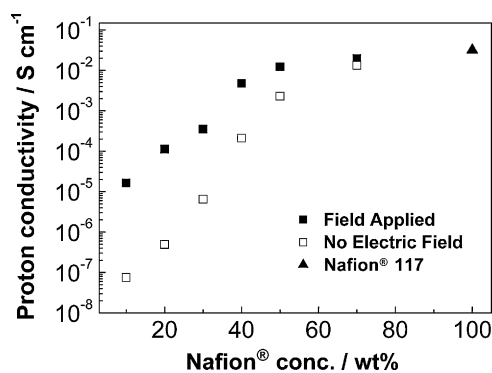

Fig. 9. Through-plane proton conductivity of Nafion®/SEBS composite membranes as a function of Nafion® content.
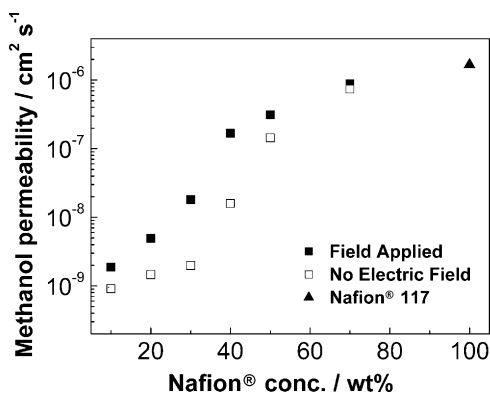
Fig. 10. Methanol permeability of Nafion®/SEBS composite membranes as a function of Nafion® content.

Fig. 11. Selectivity (defined as proton conductivity divided by methanol permeability) of Nafion®/SEBS composite membranes as a function of Nafion® content.

ity because Nafion® content is well above the percolation threshold for conductivity.

The methanol permeability of the Nafion®/SEBS composite membranes is shown in Fig. 10. All of the composite membranes have lower methanol permeability than the pure Nafion® membrane. The hydrophobic SEBS is an effective barrier to methanol, and methanol permeability decreases as the fraction of SEBS is increased. There are distinct differences in the methanol permeability versus Nafion® content for membranes prepared under the electric field compared to those without the applied field. For membranes prepared without the applied field, the methanol permeability is very low below 40 wt.% Nafion®. Above 40 wt.% Nafion®, there is a significant increase in permeability since the percolation threshold is surpassed. The theoretical threshold volume fraction was found to be 25% using a continuum percolation model [41]. This value corresponds to about 42 wt.% Nafion® in SEBS matrix. Above the percolation threshold, the Nafion® particles form an interconnected network through which methanol can diffuse. The membranes formed under the applied electric field all display higher methanol permeability than those formed without the electric field at the same Nafion® content. The particle chaining induced by the electric field provides diffusion paths for methanol to pass through the membrane, effectively lowering the threshold for percolation.

The optimal polymer electrolyte membrane for a direct methanol fuel cell application should have the lowest possible methanol permeability (P) while maintaining the highest possible proton conductivity (σ) [10]. The ratio of σ/P is defined as the membrane selectivity, and is often used as a measure of the potential effectiveness of a membrane in a DMFC. From the conductivity and permeability data shown in Figs. 9 and 10, the selectivity of the composite membranes and the Nafion® membrane was calculated and the results are plotted in Fig. 11. The particle chaining induced by the applied field causes both the proton conductivity and methanol permeability to increase compared to membranes prepared without the applied field at the same Nafion® content. However, Fig. 11 shows that the applied field causes the selectivity to be enhanced compared to membranes formed without an applied field at the same Nafion® content. Although there is some scatter in the data, several of the membranes formed under the applied field have higher selectivity than pure Nafion®. The highest measured selectivity was for 50/50 Nafion®/SEBS membrane formed under the applied field, that had a selectivity about twice as high as that of the Nafion® 117 membrane. Based on the selectivity results, the 50/50 Nafion®/SEBS membrane was chosen for testing of DMFC performance in comparison to Nafion® 117.

Three types of fuel cell membranes were investigated for DMFC performance; 50/50 Nafion®/SEBS formed under the applied elec-
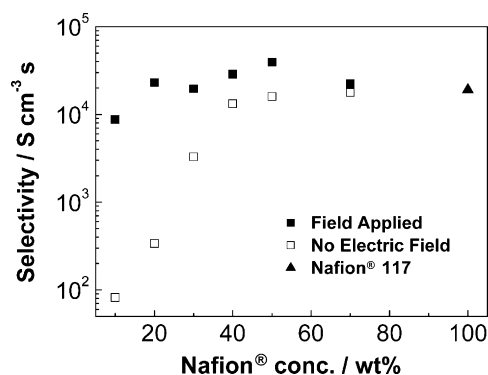
tric field, 50/50 Nafion®/SEBS formed without the applied field and Nafion® 117. To create a membrane electrode assembly (MEA), catalysts and electrodes were attached to the membranes via hot press. Since the hot pressing process may destroy the ordered structure of field-aligned membranes, the time for hot pressing was kept short, only 1 min, for the Nafion®/SEBS membranes. It was determined that the relatively mild hot pressing conditions were sufficient to create strongly adherent MEA layers on SEBS-containing membranes. However, for the Nafion® 117 MEAs prepared under the same conditions, the electrodes partially detached from the membrane at higher methanol concentration due to the swelling of Nafion®. Therefore, the Nafion® MEAs were formed by hot pressing for 3 min, which was found to be long enough to create stable MEAs.

DMFCs are expected to compete with lithium-ion batteries in portable devices due to the easy liquid fuel handing and no need for recharging, but the energy density of DMFCs is not comparable to that of lithium-ion batteries unless methanol fuel concentration is above 10 M [42]. However, low methanol concentrations are usually used in DMFCs to limit performance degradation due to fuel crossover. For the practical applications of DMFCs in portable devices, membranes are desired to enable use of high methanol concentration to reduce fuel volume as well as obtain sufficient energy density. Fig. 12 shows the cell potential versus current density at 40 °C for the DMFCs operating with methanol fuel concentrations of 2 M and 8 M. The composite membranes have a higher open circuit voltage than Nafion® 117 due to the lower methanol permeation. The performance is determined by the combined effects of proton conduction and fuel crossover. For the 2 M
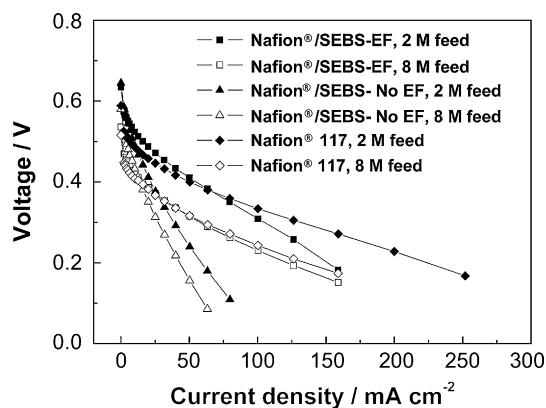

Fig. 12. Performance at 40 °C for the DMFCs made with Nafion® 117 membrane, 50/50 Nafion®/SEBS composite membrane formed under an applied field (Nafion®/SEBS-EF), and 50/50 Nafion®/SEBS composite membrane formed without an applied field (Nafion®/SEBS-No EF).

Fig. 13. Performance at 80 °C for the DMFCs made with Nafion® 117 membrane, 50/50 Nafion®/SEBS composite membrane formed under an applied field (Nafion®/SEBS-EF), and 50/50 Nafion®/SEBS composite membrane formed without an applied field (Nafion®/SEBS-No EF).
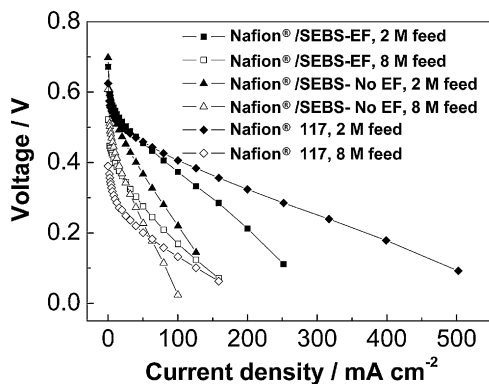
methanol feed solution, Nafion® 117 is the best performing membrane, outperforming the field-aligned Nafion®/SEBS composite, especially in the high current density range. This is likely due to the higher resistance of the MEA made with the electric field-aligned membrane, which originates from both the membrane and heterogeneous interface between the hydrocarbon membrane and the fluorocarbon Nafion® coating [43,44]. The performance of the Nafion®/SEBS-EF is far superior to that of Nafion®/SEBS-No EF. The open circuit voltage of the fuel cell is highest using the Nafion®/SEBS-No EF. However, the low proton conductivity of the membrane formed without the applied field results in a steep ohmic loss as shown in the middle part of the voltage–current curves.

With increasing methanol concentration, methanol crossover is increased while proton conduction is almost constant. As a result, the effect of methanol crossover becomes more important as methanol concentration is increased. Methanol crossover occurs due to both concentration gradient and electro-osmotic drag. The concentration diffusion dominates methanol crossover when the cell is idle, whereas electro-osmotic term is very important when the cell is operating [45]. The electro-osmotic transport depends on the methanol sorption in the membrane, especially at high methanol concentrations [46]. Nafion® 117 membranes were measured to take up ~87 wt.% methanol at room temperature when soaking them in pure methanol for 3 days, which is consistent with literature reports [28,46]. The composite membranes show significantly lower methanol sorption than pure Nafion®. The methanol uptakes of 50/50 aligned and non-aligned membranes are only about 15 wt.% and 12 wt.% respectively. Considering the previous permeability results, we can infer that the methanol crossover of composite membranes should be much less than that of Nafion® 117 in operating DMFCs. For all membranes, an increase of the methanol feed concentration lowers the open circuit voltage. As for Nafion® 117, increasing methanol concentration causes a dramatic decrease in the open circuit voltage and performance because of Nafion®'s high methanol crossover. Also, methanol permeability and electro-osmotic drag coefficient in Nafion® has been reported to increase with increasing methanol concentration and temperature [15,47,48]. As a result, the composite membranes with lower crossover have a relative improvement in performance over pure Nafion® at high methanol concentration. When the methanol feed concentration is increased to 8 M, the fuel cell with the Nafion®/SEBS-EF displays comparable performance to the fuel cell with the Nafion® 117 membrane.

When temperature is increased to 80 °C, as shown in Fig. 13, the relative performance of the different types of membranes is similar to that at 40 °C. The fuel cell with the Nafion® 117 mem-

brane is the best performing with 2 M methanol feed, while the fuel cell with the Nafion®/SEBS-EF is the best performing with 8 M methanol feed. When both temperature and methanol concentration are increased, the proton conductivity increases with temperature and methanol crossover increases with both temperature and concentration. However, the increase in methanol crossover is larger relative to the decrease in membrane resistance. The performance therefore mainly depends on the effect of fuel crossover rather than proton conduction. The electric field processed membrane shows the best performance at 8 M methanol as a result of its low methanol crossover relative to moderate proton conductivity. The membrane prepared without electric field shows poor performance because of its quite low proton conductivity.

4. Conclusions

The structure of Nafion®/SEBS membranes was successfully altered by solvent casting under an applied electric field to enhance performance in direct methanol fuel cells. It was found that field induced structure provided enhanced proton conductivity at the expense of increased methanol permeability. However, the selectivity (defined as proton conductivity divided by methanol permeability) was increased by the electric field-induced structure. Composite membranes consisting of 50% Nafion® by weight prepared without the applied electric field displayed poor performance in DMFCs. The structure induced by the applied electric field caused a significant enhancement in fuel cell performance. The 50 wt.% Nafion®/SEBS-EF exhibited better performance than the commercial Nafion® 117 when using high methanol feed concentration at high temperature. The structure induced by the electric field also resulted in anisotropic swelling of the membrane. Reduced area expansion of the membrane could potentially reduced stress that leads to electrode delamination from membranes in fuel cells undergoing humidity cycling. Moreover, these anisotropic membranes are easy to prepare and less expensive than the pure Nafion® membrane.

References

[1] M. Waidhas, W. Drenckhahn, W. Preidel, H. Landes, J. Power Sources 61 (1996) 91–97.
[2] J. Ge, H. Liu, J. Power Sources 142 (2005) 56–69.
[3] G. Alberti, M. Casciola, Solid State Ionics 145 (2001) 3–16.
[4] V. Neburchilov, J. Martin, H. Wang, J. Zhang, J. Power Sources 169 (2007) 221–238.
[5] N.W. Deluca, Y.A. Elabd, J. Polym. Sci., Part B: Polym. Phys. 44 (2006) 2201–2225.
[6] V.S. Silva, B. Ruffmann, S. Vetter, A. Mendes, L.M. Madeira, S.P. Nunes, Catal. Today 104 (2005) 205–212.
[7] V. Tricoli, J. Electrochem. Soc. 145 (1998) 3798–3801.
[8] J. Wootthikanokkhan, N. Seeponkai, J. Appl. Polym. Sci. 102 (2006) 5941–5947.
[9] P. Dimitrova, K.A. Friedrich, U. Stimming, B. Vogt, Solid State Ionics 150 (2002) 115–122.
[10] J.P. Shin, B.J. Chang, J.H. Kim, S.B. Lee, D.H. Suh, J. Membr. Sci. 251 (2005) 247–254.
[11] B. Smitha, S. Sridhar, A.A. Khan, J. Membr. Sci. 225 (2003) 63–76.
[12] C.H. Lee, K.A. Min, H.B. Park, Y.T. Hong, B.O. Jung, Y.M. Lee, J. Membr. Sci. 303 (2007) 258–266.
[13] C.H. Rhee, H.K. Kim, H. Chang, J.S. Lee, Chem. Mater. 17 (2005) 1691–1697.
[14] S.W. Choi, Y.Z. Fu, Y.R. Ahn, S.M. Jo, A. Manthiram, J. Power Sources 180 (2008) 167–171.
[15] J. Lin, J.K. Lee, M. Kellner, R. Wycisk, P.N. Pintauro, J. Electrochem. Soc. 153 (2006) A1325–A1331.
[16] C. Gehin, J. Persello, D. Charraut, B. Cabane, J. Colloid Interface Sci. 273 (2004) 658–667.
[17] T.B. Jones, Electromechanics of Particles, Cambridge University Press, Cambridge, 1995.

[18] B. Khusid, A. Acrivos, Phys. Rev. E: Stat., Nonlinear, Soft Matter Phys. 54 (1996) 5428–5435.
[19] M. Parthasarathy, D.J. Klingenberg, Mater. Sci. Eng., R 17 (1996) 57–103.
[20] C.P. Bowen, R.E. Newnham, C.A. Randall, J. Mater. Res. 13 (1997) 205–210.
[21] G. Kim, Y.M. Shkel, J. Mater. Res. 19 (2004) 1164–1174.
[22] Y. Oren, V. Freger, C. Linder, J. Membr. Sci. 239 (2004) 17–26.
[23] V. Tomer, C.A. Randall, G. Polizos, J. Kostelnick, E. Manias, J. Appl. Phys. 103 (2008) 034115.
[24] D. Liu, M.Z. Yates, J. Membr. Sci. 322 (2008) 256–264.
[25] D. Liu, M.Z. Yates, J. Membr. Sci. 326 (2009) 539–548.
[26] J. Kim, B. Kim, B. Jung, J. Membr. Sci. 207 (2002) 129–137.
[27] A. Matsuda, N. Nakamoto, K. Tadanaga, T. Minami, M. Tatsumisago, Solid State Ionics 177 (2006) 2437–2441.
[28] D. Sangeetha, Eur. Polym. J. 41 (2005) 2644–2652.
[29] C.H. Lee, H.B. Park, Y.M. Lee, R.D. Lee, Ind. Eng. Chem. Res. 44 (2005) 7617–7626.
[30] Z. Xie, C. Song, B. Andreaus, T.I. Navessin, Z. Shi, J. Zhang, S. Holdcroft, J. Electrochem. Soc. 153 (2006) E173–E178.
[31] S. Gottesfeld, X. Ren, P. Zelenay, J. Davey, S.C. Thomas, P. Storm (2004).
[32] S. Wang, G. Sun, G. Wang, Z. Zhou, X. Zhao, H. Sun, X. Fan, B. Yi, Q. Xin, Electrochem. Commun. 7 (2005) 1007–1012.
[33] S.J. Paddison, D.W. Reagor, T.A. Zawodzinski, J. Electroanal. Chem. 459 (1998) 91–97.
[34] S. Butkewitsch, J. Scheinbeim, Appl. Surf. Sci. 252 (2006) 8277–8286.
[35] W.R. Pyle, Phys. Rev. 38 (1931) 1057–1070.
[36] L. Zhang, S. Mukerjee, J. Electrochem. Soc. 153 (2006) A1062–A1072.
[37] S.H. de Almeida, Y. Kawano, J. Therm. Anal. Calorim. 58 (1999) 569–577.
[38] T. Yamaguchi, F. Miyata, S. Nakao, J. Membr. Sci. 214 (2003) 283–292.
[39] K.D. Kreuer, J. Membr. Sci. 185 (2000) 29–39.
[40] H.Y. Jung, J.K. Park, Electrochim. Acta 52 (2007) 7464–7468.
[41] S. Kirkpatrick, Rev. Mod. Phys. 45 (1973) 574–588.
[42] Y.H. Pan, Electrochem. Solid-State Lett. 9 (2006) A349–A351.
[43] B. Bae, D. Kim, J. Membr. Sci. 220 (2003) 75–87.
[44] H.J. Kim, J.E. Lim, Y.G. Shul, H. Han, Stud. Surf. Sci. Catal. 154 (2004) 3036–3043.
[45] J. Ling, O. Savadogo, J. Electrochem. Soc. 151 (2004) A1604–A1610.
[46] D.T. Hallinan, Y.A. Elabd, J. Phys. Chem. B 111 (2007) 13221–13230.
[47] B.S. Pivovar, Y. Wang, E.L. Cussler, J. Membr. Sci. 154 (1999) 155–162.
[48] T. Tschinder, T. Schaffer, S.D. Fraseer, V. Hacker, J. Appl. Electrochem. 37 (2007) 711–716.